



Supplement of

Investigation of near-global daytime boundary layer height using high-resolution radiosondes: first results and comparison with ERA5, MERRA-2, JRA-55, and NCEP-2 reanalyses

Jianping Guo et al.

Correspondence to: Jian Zhang (zhangjian@cug.edu.cn)

The copyright of individual parts of the supplement might differ from the article licence.

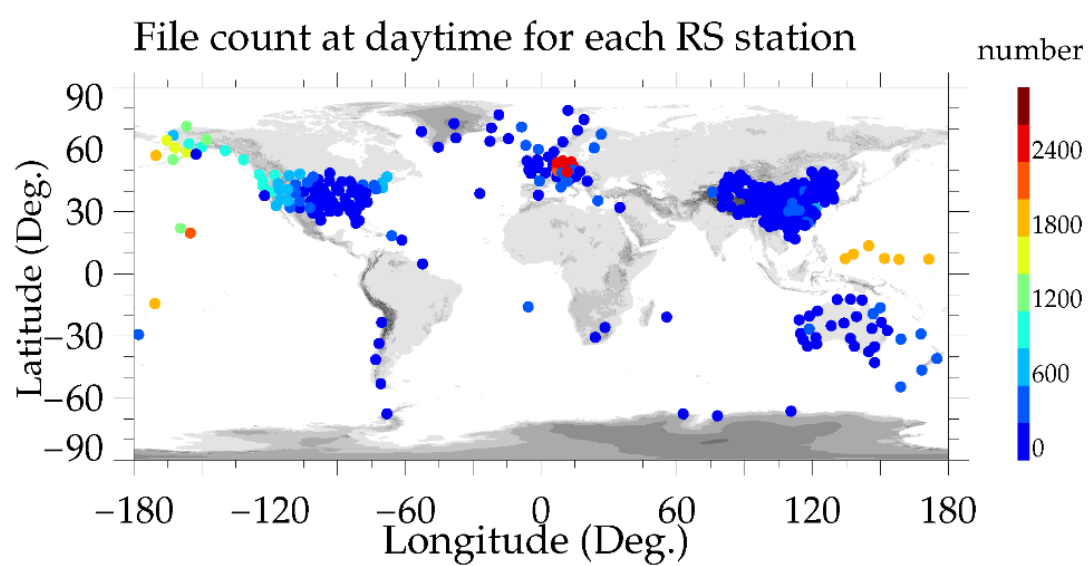


Figure S1. Profile count of radiosonde station in the daytime.

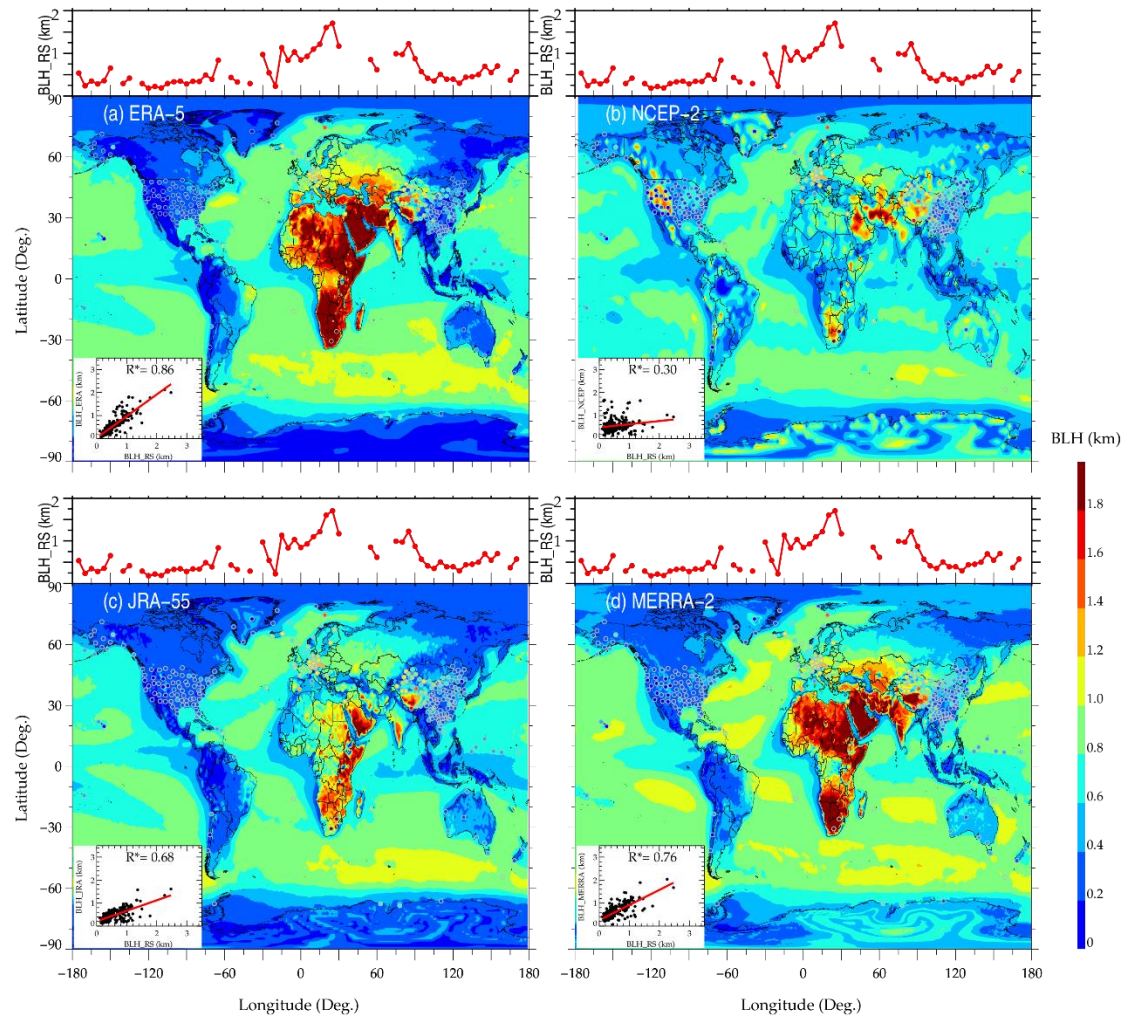


Figure S2. Mean BLH estimated from ERA-5 (a), NCEP-2 (b), JRA-55 (c), and MERRA-2 (d) reanalysis data at 1200 UTC during the years 2012-2019. The dots with gray marginal lines in each map denote the mean BLH derived by sondes at 1200 UTC. The station with less than 10 profiles are not included for further analysis. The 2D scatter plot in the left bottom of each panel illustrates the correlations between reanalysis-derived and sonde-derived BLHs at 1200 UTC, where the star superscripts indicate that the correlation coefficients are statistically significant ($p < 0.05$) and the red lines show a linear fit.

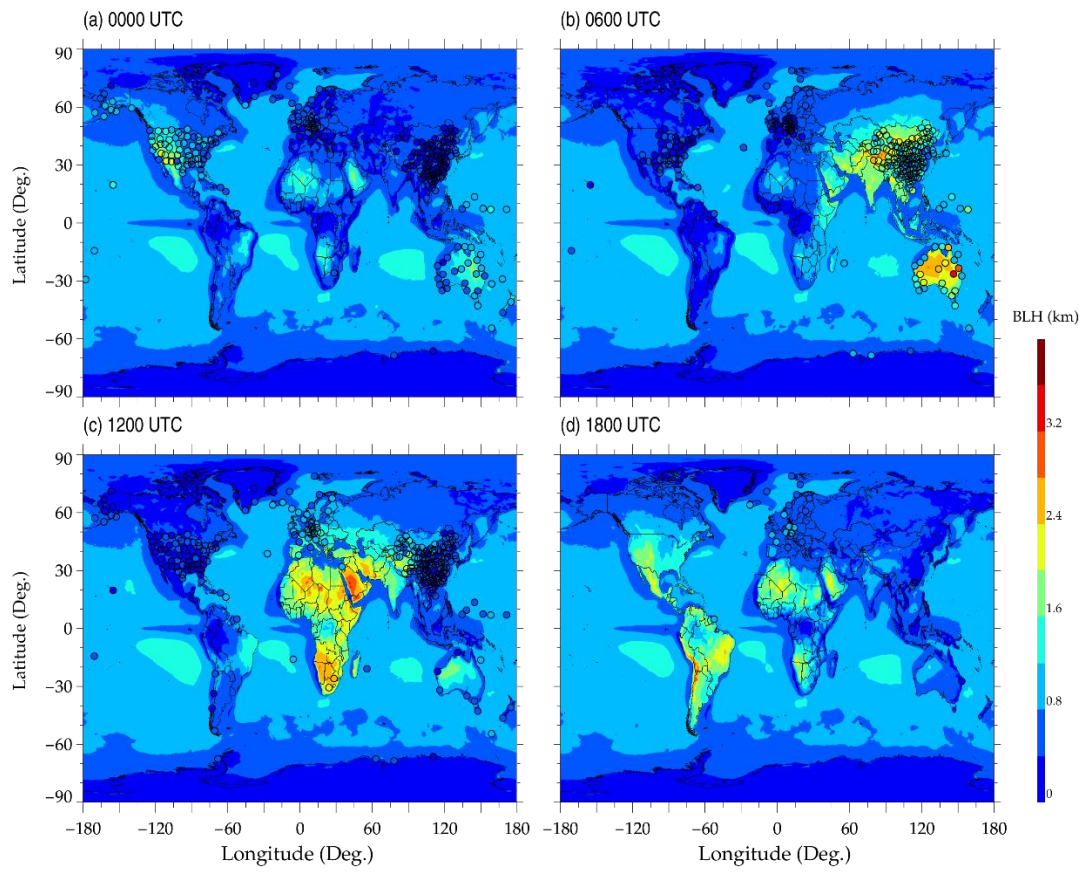


Figure S3. The mean packaged BLH in MERRA-2 at (a) 0000 UTC, (b) 0600 UTC, (c) 1200 UTC, (d) 1800 UTC during years 2012 – 2019. The dots with gray marginal lines in each map denote the mean BLH derived by sondes.

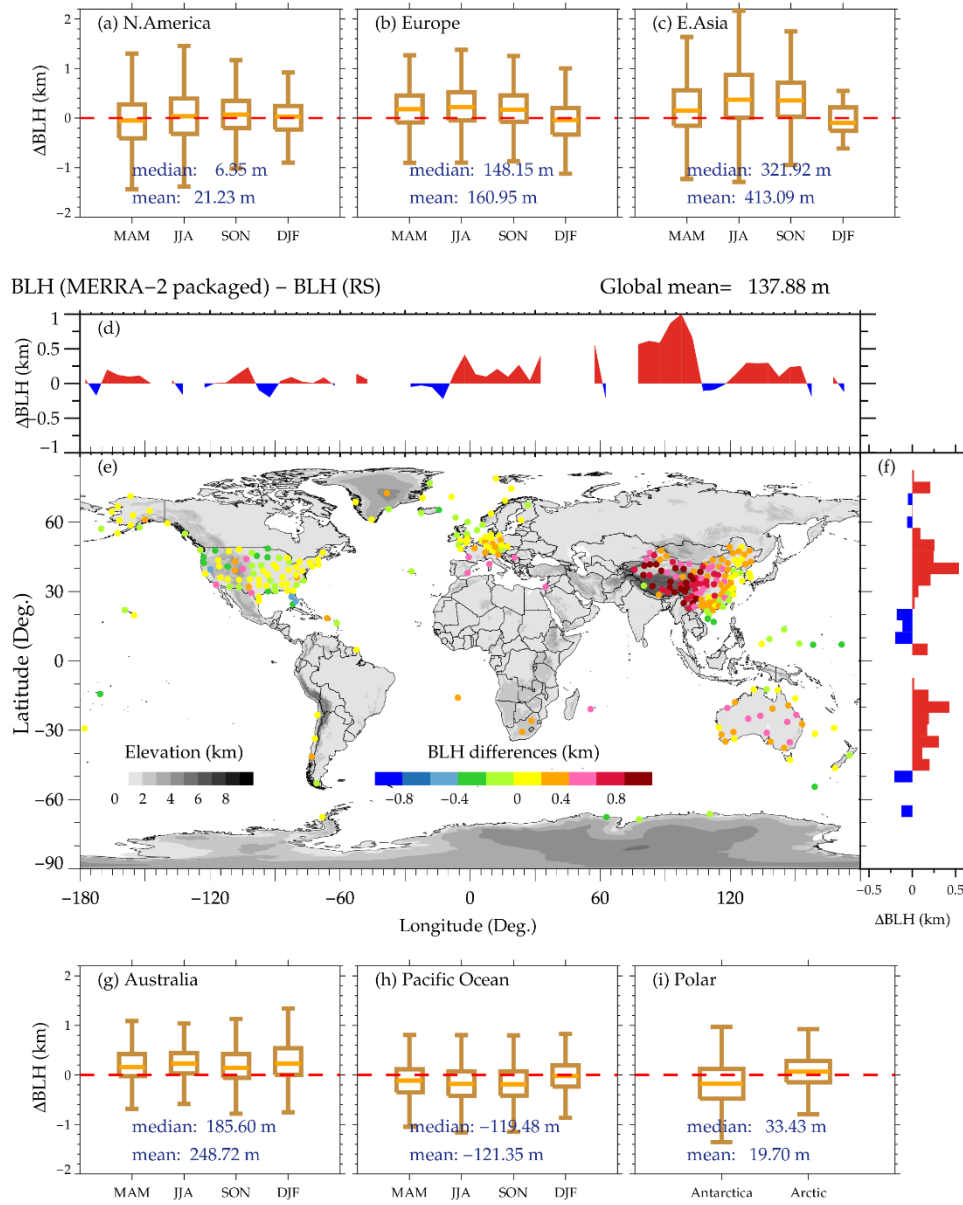


Figure S4. Differences between BLH(RS) and BLH(MERRA2_packaged). The spatial distribution of mean differences is highlighted in (e). Also shown are the distributions of mean BLH differences as a function of longitude (d) and latitude (f). The box and whisker plot of BLH differences over the six regions of interest (i.e., North America, Europe, East Asia, Austria, Pacific Ocean, Polar) over four seasons are displayed in (a-c), (g-i). The seasons are defined as follows: MAM, March–April–May; JJA, June–July–August; SON, September–October–November; DJF, December–January–February.